Analytical Methods

Accepted Manuscript

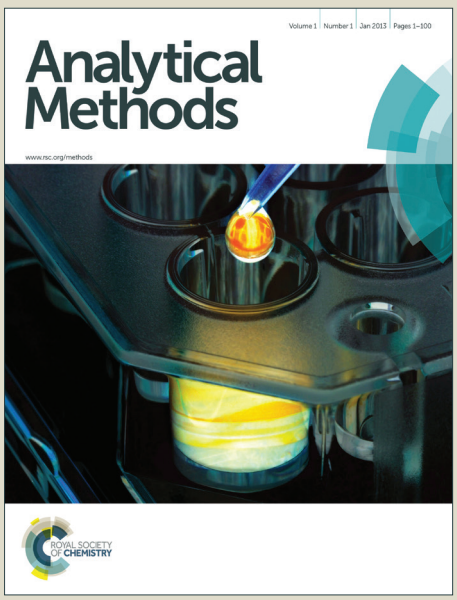

ROYAL SOCIETY OF CHEMISTRY

www.rsc.org/methods

Cite this: DOI: 10.1039/c0xx00000x

www.rsc.org/xxxxxx

ARTICLE TYPE

Diffuse reflectance FTIR database for the interpretation of the spectra obtained with a handheld device on Built Heritage materials

Iker Arrizabalaga,*[a] Olivia Gómez-Laserna,[a] José Antonio Carrero,[a] Julen Bustamante,[a] Azibar Rodríguez,[a] Gorka Arana[a] and Juan Manuel Madariaga[a]

Received (in XXX, XXX) Xth XXXXXXXXX 20XX, Accepted Xth XXXXXXXXX 20XX
DOI: 10.1039/b000000x

FTIR handheld devices, working in the Diffuse Reflectance mode (DRIFT), are promising analytical instruments to perform in situ analyses in Cultural Heritage materials. However, in the analyses performed in-situ with the such DRIFT handheld device distortions in the DRIFT spectra can be observed in the measurements due to the presence of specular reflection, showing inverted bands on those IR bands with the highest absorption index. These distortions present in the spectra obtained with handheld devices make their resolution very difficult unless the working mode of the devices is well known and a suitable DRIFT database is available. With the aim of getting the most suitable tools to perform analyses in the field, this work has been developed considering two important aspects. In the first one, the differences between the spectra obtained in transmittance, attenuated total reflectance and diffuse reflectance of some compounds (nitrates, sulphates and carbonates), that could show the inverted bands when are measured with the FTIR handheld device have been studied. In the second one, a preliminary database of several compounds that can be found as original (bulk) compounds or as efflorescence in affected Built Heritage materials, obtained in the laboratory in diffuse reflectance mode, is presented. Finally, the usefulness of the presented database has been tested with spectra obtained in situ in the Fishermen's association building (San Sebastian, Basque Country, North of Spain) on areas presenting several decaying processes.
.

1. Introduction

In the recent years, portable equipments have experienced a great development, especially in the field of molecular spectroscopy[1]. Fourier Transform Infrared spectroscopy (FTIR) and Raman spectroscopy are the most used techniques to perform the in situ analyses in Cultural Heritage materials. Unfortunately, many of the samples analyzed contain chromophore compounds or organic matter, which could produce a high fluorescence making the analysis by Raman spectroscopy more difficult[2]. Therefore, when the analyzed matrices show fluorescence with Raman spectroscopy, FTIR becomes a very useful technique.

In the literature, several works can be found analyzing materials in-situ with non-invasive infrared reflectance equipments. Most of them have been performed with Fibre Optic Reflectance Spectroscopy (FORS) in which different kinds of analyses have been carried out in several materials, such as, pigments[3-4], binders[5], wooden materials[6], calcarenites and marbles[7].

In the measurements performed in situ by FORS or DRIFT handheld devices the biggest drawback is that diffuse component cannot be optically separated from specular one and this interaction is the main source of distortions[8]. The specular reflectance is ruled by de Fresnel equation and depends on the refractive index (n) and absorption index (k) of the analyzed material. In the case of specular reflection, two types of spectral distortion can happen, the first one, when the sample has k<1 the spectra is characterized by a derivative-like features. The second type of distortion can appear when the sample contains a compound with a k >>1. In these cases, Reststrahlen bands[9] appear and this happens with most inorganic salts containing oxyanions such as carbonates, sulphates, nitrates, silicates, and oxalates[10-11].

Therefore, when samples with k >>1 are measured with FORS or DRIFT handheld devices distorted spectra will be obtained. These distortions are directly related with the detection of the specular reflectance, thus an optical configuration that minimizes the detection of specular reflectance would be the best to obtain less distorted spectra.

As can be read in the literature, generally, the majority of the limitations of the FORS could come from the optical geometry that works at 0º in – 0º out, where incident radiation is sent perpendicular to the sample and total reflectivity is collected at

the same angle in the same direction[12]. This optical configuration favours the collection of the specular reflectance and theoretically, the obtained spectra will be distorted since the specular reflectance component will be predominant in the detected total reflectance signal.

In contrast, in a recent publication, the applicability of a Diffuse Reflectance Infrared Fourier Transform (DRIFT) handheld spectrometer to perform in-situ analyses has been tested[13]. With this handheld device the IR radiation is emitted at 0º (perpendicular to the surface) and the reflected signal is collected inside an imaginary cone of 45 ° around the emission beam. With this optical configuration, the optical head measures a higher proportion of the diffuse reflectance signal and a lower proportion of the specular one, obtaining very good results[13-15], although the distortions mentioned above still appear in the spectra.

In the work presented by Aramendia et al[16], a very interesting situation related with the reflectance spectroscopy is exposed. This paper studies the dissolution process of weathering steel in urban areas. In the work some spectra obtained in situ with the handheld device can be seen. What really matters in this work is that in any of these spectra taken in situ, an inverted bands originated by the Reststrahlen effect can be seen. In these special samples, the surface was so rough that the only component detected was the diffuse reflectance and the obtained spectra did not show any distortion, in spite of being obtained in situ by reflectance spectroscopy. Hence, the spectra obtained in situ with FORS or with de DRIFT handheld devices will be completely dependent to the detection of the specular reflectance.

The distortions present in the spectra obtained with the DRIFT handheld device make the interpretation of the IR spectra very difficult especially when several compounds are present. Diffuse reflectance (DR) spectroscopy makes the width of the sample appear larger. In the sample many reflections take place and, as a consequence, overtones (integral multiples of the fundamental absorption frequencies) and combination bands (addition and subtraction of the fundamental absorption frequencies) increase their signals[17]. Owing to these enhancements present in the spectra obtained in situ, the bands that have increased their intensity may be the key to perform a correct resolution (assignation to unknown compounds) of the spectra.

In 2006 a preliminary DR database of 24 dyes and pigments commonly used in painting and artworks was published[18]. In that work, Silva et al. a comparative study between transmittance and diffuse reflectance was performed. The benefits of the diffuse reflectance mode were exposed and the problems that could arise during the measurements in the laboratory were studied. In this way, 24 compounds were measured using both modes (transmittance and DR) and plotted % of transmittance versus Kubelka-Munk units. When a reflectance spectrum is converted to Kubelka-Munk units, the obtained spectrum is similar to that obtained in transmittance mode, as we can see in the work presented by Silva et al. However, if we compare a spectrum obtained with the handheld device and one obtained in transmittance, attenuated total reflectance (ATR) or DR mode, the differences between them are quite clear, as will be shown in this work.

For this reason, this work has been carried out with two main purposes. The first one is to study the spectra obtained with different IR modes (transmittance, ATR and DR) of some compounds that can show Reststrahlen effect when they are measured in situ and select the best procedure to resolve the spectra obtained with the handheld device. The second purpose would be to present a preliminary database of some compounds, usually found in efflorescence of impacted Built Heritage materials, obtained in the laboratory in DR mode, in order to get the best tool for the resolution of the spectra obtained with a DRIFT handheld device. These compounds are interesting as they can be found in the pathologies described for Cultural Heritage materials.

2. Experimental

The laboratory equipment was a Jasco 6300 FTIR spectrophotometer equipped with three different attachments. The first one, for standard transmittance measurements, the second one for diffuse reflection measurements (Jasco DR PR0410M) and the last one, for measurements in ATR mode (PIKE Miracle $_{tm}$).The equipment has a Michaelson interferometer at maximum resolution of 0.07 cm^{-1} and a Ge/KBr beam splitter with a DLATGS detector with Peltier temperature control. All transmittance and DR spectra obtained in the laboratory were collected in the middle infrared region (from 4000 to 400 cm^{-1}) recording 32 scans per spectrum at a spectral resolution of 4 cm^{-1}. The ATR spectra were collected also in the middle infrared region (from 4000 to 650 cm^{-1}) recording 32 scans per spectrum at a spectral resolution of 4 cm^{-1}.

KBr powder was used as background and as diluent for the transmittance and DR measures in the laboratory. For the DR analyses, all samples and standards were dispersed in KBr at proportions between 5% and 10%, depending on the compound and grinded in a particle size smaller than 10 μm to avoid distortions. Finally, the obtained mixtures were placed in the microsample cup to be measured. Dilution of the sample generates less specular component in the surface of the sample, thereby increasing the contribution of the diffuse reflectance component. For the transmittance measurements, 0.2-0.5 mg of sample was dispersed in 200 mg of KBr.

Laboratory non invasive and in situ diffuse reflectance spectra were acquired with a 4100 Exoscan handheld FTIR spectrometer (Agilent) with a diffuse reflectance sampling interface recording short acquisition times and 32 accumulations. The Michaelson interferometer has a maximum resolution of 4 cm^{-1} and a maximum spectral range of 4000–600 cm^{-1}. The system has a ZnSe beam splitter and a DTGS detector. The background was acquired with a diffuse gold reference cap. In both cases, analysis and the spectra treatment were performed using Nicolet Omnic 7.2 software (Madison, WI, USA).

The origin of the standards that have been characterized by diffuse reflectance in the laboratory is the following:

Nonahydrated aluminium nitrate (Merk 98.5%), aluminium sulphate (Aldrich 99.9%), ammonium sulphate (Sigma, 99%), lead (II) sulphate (Aldrich 98%), lead (II) nitrate (Sigma-Aldrich 99%), iron (II) sulphate (Merck 99.5), nonahydrated iron (II) nitrate (Merck 98%), calcium carbonate (Sigma Aldrich 99%), tetrahydrated calcium nitrate (Merck 98.5%), dehydrated calcium sulphate (Fluka 99%), hexahydrated magnesium nitrate (Sigma Aldrich 98%), magnesium sulphate (Fluka 98%), potassium nitrate (Sigma Aldrich 99%), potassium sulphate (Riedel-deHaen 99%), sodium carbonate (Merck 99.9), sodium nitrate (Fluka 98%), sodium sulphate (Sigma Aldrich 99%), silicon oxide (Kremer 97%) and calcium oxalate monohydrated (Panreac 98%).

3. Study of the spectra obtained by Transmittance, ATR, DR and by the FTIR handheld device in the laboratory

As mentioned in the introduction, in this section the different spectra obtained with transmittance, ATR, DR and the handheld device on samples that can show Reststrahlen effect (nitrate, sulphate and carbonate) have been studied. To illustrate the importance of a good database, some spectra obtained in the laboratory with the handheld device were resolved using spectra of standard compounds measured in transmittance, ATR and as well as DR mode.

3.1. Potassium nitrate

In Figure 1 the spectra obtained by transmittance, ATR, DR and with the handheld device can be seen. As is usually done in the literature, the transmittance spectrum was plotted in % of transmittance and the ATR spectrum was plotted in % of reflectance. The spectra obtained in DR mode and with the handheld device were plotted in log (1/R) units.

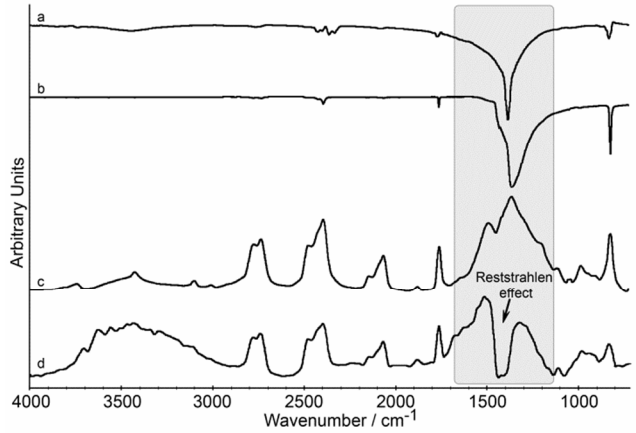

Fig. 1 Spectrum of potassium nitrate (region 4000-700cm^{-1}): a) transmittance, b) ATR, c) DR and d) with the handheld device

As can be seen in Figure 1, there are clear differences between Transmission, ATR and DR spectra. To explain the differences between the spectra it is necessary to understand the measurement conditions and the processes involved.

Transmission spectroscopy is explained by the well known Lambert-Beer's equation[19]. In this mode, the IR radiation is emitted through a KBr pellet, and the obtained spectrum is the graphic representation of the relation between the intensity of emitted and received light. By contrast, ATR is a surface examination technique and an internal reflecting element is used to focus and direct the light to the sample. The IR radiation penetrates about 1-5 μm into the sample, is absorbed, then the light is reflected to the crystal and finally reaches the detector. The ATR mode works with effective thickness (d_e) and depth of penetration (dp) as was explained by Harrick and Averett[20-21].

The theories behind these techniques are different and, as was expected, the output spectra look different. As can be seen in Figure 1, the transmittance spectrum is a typical spectrum obtained in transmittance mode, in which the main band is narrow and well defined. In contrast, the ATR spectrum looks more distorted and the main band is shifted to lower frequencies. In the literature band shifts between 1-50 cm^{-1} in the MIR region can be found[22].

If we compare the transmittance and the ATR spectra, we could see that, there is a shift of 20 cm^{-1} in the main band. In the case of the transmittance spectrum, the main band appears at 1384cm^{-1} and in the ATR spectrum at 1364cm^{-1}. Nevertheless, this change in position of the main band it is not relevant for our purpose, because if we look at the spectra obtained with the handheld device (Figure 1), the shaded region that can be seen around 1200-1650cm^{-1} is distorted by the Reststrahlen effect. Thus, this area is not useful to perform the resolution of the spectrum. If we look at the secondary bands in the ATR spectrum, we can see other three bands at 823, 1762 and 2395 cm^{-1} that could be used for the resolution of the spectrum. Nevertheless, in the transmittance spectrum we can see only two of the bands mentioned above, the first one at 823 cm^{-1} and the second one at 1762 cm^{-1}. Therefore, using the transmittance and ATR spectra we can only assign correctly 2-3 of the bands that can be seen in the spectrum obtained with the handheld device.

This situation was expected since the FTIR handheld device measures the total reflectance on the surface of the sample. As we have seen, the interaction of the specular and diffuse reflectance has created an inverted band in the analyzed spectrum, although it is still possible to identify correctly five bands using the standard DR spectrum.

Diffuse reflection is originated from an absorption process and, unlike internal attenuated total reflection (ATR), diffuse reflection spectroscopy lacks an exact theoretical description[23]. In the measurements performed in DR mode, the IR radiation penetrates the sample and inside the sample a high number of refractions and absorption processes take place. For this reason, in the diffuse reflectance spectra an enhancement of the intensity in the weak IR bands is observed[24].

Hence, the best spectrum to resolve the distorted spectrum obtained with the handheld device on a potassium nitrate sample is the standard obtained in the laboratory in DR mode. With this

standard it is possible to assign correctly 5 bands instead of 2 or 3 that could be identified using the transmittance and ATR standards. In the spectra obtained in the laboratory in DR mode, there is no Reststrahlen effect, since the sample was ground and diluted in order to reduce the specular component[17].

If we analyze the features of the obtained spectra, we can see that that the number of reflections that happen inside the sample modifies the shape of the spectra. In the transmittance spectra, the IR radiation is emitted through a KBr pellet and a single absorption is given. Thus, the obtained IR bands are usually narrow and well defined. In contrast, in reflectance measurement, a high number of reflections and absorption processes take place and depending on the mode in which the measurements are carried out, the obtained spectral features will be different. In the DR analyses, an enhancement of the intensity in the weak IR bands is observed and also an increase in the bandwidth of the main band, as can be seen in the figure 1. In the ATR measurements, in spite of being a reflectance measurement it was not seen an enhancement of the intensity in the weak IR bands, but an increase of the bandwidth of the main band is observed.

Comparing the spectrum obtained in DR mode and that obtained with the handheld device, we can conclude that the both spectra are very similar. The only difference is the distortion present in the spectra obtained with the handheld device created by the Reststrahlen effect. Finally, thanks to the dilution with KBr the samples and standards in the DR measurements have not led to any problems in the comparison with spectra obtained with the handheld device, as can be seen in Figure 1.

3.2. Potassium sulphate

In Figure 2, the spectrum obtained by transmittance, ATR, DR and with the handheld device on a potassium sulphate sample can be seen. The spectrum obtained with the handheld device shows the following IR bands: 727, 1551, 1602, 2061, 2142, 2207 and 2266 cm^{-1}.

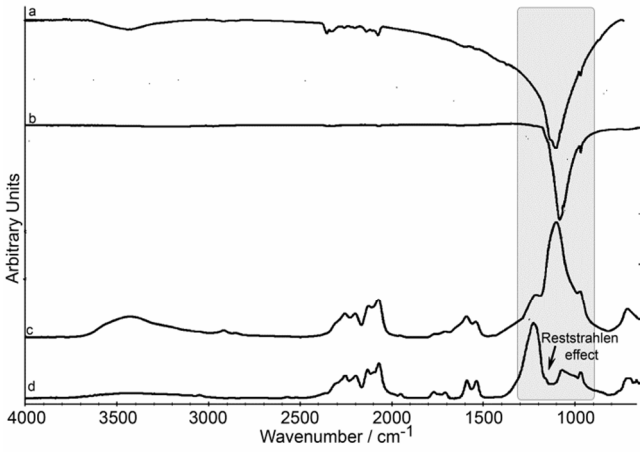

Fig. 2 Spectrum of potassium sulphate (region 4000-700cm^{-1}): a) transmittance, b) ATR, c) DR and d) with the handheld device

In Figure 2, clear differences between Transmission, ATR and DR spectra can be observed again. Analyzing the spectra obtained in the same way as in the previous case, we could see that, there is a shift of 20cm^{-1} in the main band between the spectra obtained in transmittance and ATR mode. In the case of the transmittance spectrum, the main band appears at 1117 cm^{-1} and in the ATR spectrum at 1097 cm^{-1}. This change in position of the main band is not relevant for our purpose as before, because, in the spectrum obtained with the handheld device (Figure 2), the region around 900-1300 cm^{-1} is distorted by the Reststrahlen effect and this area is not useful to perform the band assignation to given compounds. In addition, in the transmittance spectrum (Figure 2) we can see other two weak bands at 2061 and 2142 cm^{-1} that could be used for the resolution of the spectrum. However, in the ATR spectrum (Figure 2), we cannot see any band outside the region distorted by the Reststrahlen effect. Accordingly, using the ATR spectrum it would be impossible to resolve the spectrum obtained with the handheld device and performing the resolution by using the spectrum obtained in transmittance mode would be a difficult task.

On the contrary, looking at the DR spectrum, we can see seven bands at 727, 1551, 1602, 2061, 2142, 2207 and 2266 cm^{-1} outside the distorted region by the Reststrahlen effect that match most of the IR bands obtained with the handheld instrument. Therefore, using a standard in DR mode to resolve the spectrum obtained with the handheld device, makes the work easier.

Once we have resolved the spectrum obtained with the handheld device, it would be interesting to analyze the band at 1241cm^{-1}. In this case, we knew that the sample was a potassium sulphate and we were expecting an inverted band caused by the Reststrahlen effect. However, if the analyzed sample was unknown and we had to resolve the spectrum, we should be careful with this band. If we observe only the spectrum obtained with the handheld device, we might think that it is a typical IR spectrum and the analyzed compound has the main band at 1241 cm^{-1}. Nonetheless, this band is related to the weak band that can be seen at 1241 cm^{-1} in the DR spectrum in Figure 2, which has greatly increased its intensity.

3.3. Calcium carbonate

In Figure 3, the spectra obtained by transmittance, ATR, DR and with the handheld device on a calcium carbonate sample. The spectrum obtained with the handheld device shows the following IR bands: 711, 873, 1794, 2514, 2868 and 2972 cm^{-1}.

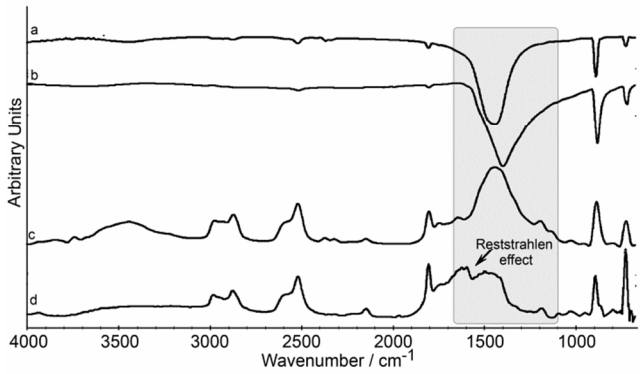

Fig. 3 Spectrum of calcium carbonate (region 4000-700cm^{-1}): a) transmittance, b) ATR, c) DR and d) with the handheld device.

If we study the spectra obtained, a shift of 40cm^{-1} in the main band can be observed, between the spectra obtained in transmittance and ATR mode. In the case of the transmittance spectrum, the main band appears at 1427cm^{-1} and in the ATR spectrum at 1387 cm^{-1}. As has happened in the previous cases, the spectrum obtained with the handheld device (Figure 3) is distorted by the Reststrahlen effect and the region around 1050-1600 cm^{-1} is not useful to perform the resolution of the spectrum. In the transmittance and DR spectra six bands at 711, 873, 1794, 2514, 2868 and 2972 cm^{-1} can be seen. In contrast, in the ATR spectrum only four bands at 711, 873, 1794 and 2514 cm^{-1} can be seen. Therefore, in this case we could resolve the spectrum obtained with the handheld device using any one of the spectra obtained in the laboratory, although the bands in DR are higher and the identification is easier in this mode.

3.4. Mixed compounds

The identification of the last spectrum has been easy comparing with the previous ones and we may think that for the carbonate samples any standard in transmittance or ATR mode could be enough to resolve the spectra obtained with the handheld device. To demonstrate the usefulness of a good database in DR mode we prepared binary mixtures (1:1) with compounds that can show inverted bands.

The first mixed spectrum analyzed was obtained with the handheld device on a potassium nitrate and potassium sulphate sample. In Figure 4, the obtained spectrum (a) shows the following IR bands: 724, 842, 1761, 2078, 2143, 2205, 2264, 2394, 2735, 2779, 3103, 3426 and 3745 cm^{-1} outside the region distorted by the Reststrahlen effect.

Apart from the distortions presented in the spectrum, it was very likely to have some areas where the bands of the two compounds were overlapped, which makes more difficult the resolution of the spectrum. The bands that can be seen in the region around 2000-2200 cm^{-1} belong to both compounds, thus, this area cannot be used for the resolution of the spectrum obtained with the handheld device. The assignation of the potassium nitrate was simple since 8 bands (842, 1761, 2394, 2735, 2779, 3103, 3426 and 3745cm^{-1}) match perfectly between the analyzed spectrum and the DR standard spectrum.

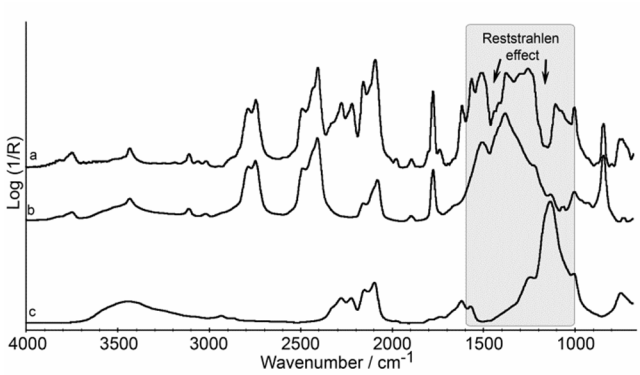

Fig. 4 a) Spectrum obtained with the handheld device in the region 4000-700cm^{-1} on potassium nitrate and potassium sulphate sample, b) DR spectrum obtained in the region 4000-700cm^{-1} on potassium nitrate sample and c) DR spectrum obtained in the region 4000-700cm^{-1} on potassium sulphate sample

Going back to the assignation of the potassium sulphate, we can see that, in this case, there are four bands to perform the assignation (724, 1602, 2205 and 2264 cm^{-1}), in contrast, in the second example with pure potassium sulphate (Figure 2) the assignation was carried out with 7 bands (727, 1551, 1602, 2061, 2142, 2207 and 2266 cm^{-1}). Therefore, when mixtures of compounds that show inverted bands are analyzed, the use of the secondary bands to perform the resolution of the spectrum obtained with the handheld becomes necessary.

With the aim of getting an even a more complex spectrum, a mixture of calcium carbonate and anhydrous sodium carbonate was analyzed. In Figure 5, the obtained spectrum (a) shows the following IR bands: 750, 881, 1784, 2506, 2593, 2873 and 2971 cm^{-1} outside the region distorted by the Reststrahlen effect.

If the analyzed spectrum was an unknown sample, it would be clear that the analyzed spectrum belongs to a carbonate sample, but if we wanted to know exactly the composition of the sample the resolution of the spectrum would be really difficult, as we will see.

As in the previous case, apart from the distortions present in the spectrum (1100-1500cm^{-1}), there are some areas where the bands of the two compounds were overlapped. For example, in the spectrum a of Figure 5, in the area around 700-900cm^{-1}, two bands at 705 and 881 cm^{-1} can be observed. With these bands, it is very difficult to say which band belongs to each compound since both bands seems to be overlapped. The calcium carbonate standard shows bands at 711 and 873cm^{-1} and sodium carbonate at 690 and 870cm^{-1}. In both spectra, the second band appears in the same place and it is not useful to discern between both carbonates. In contrast, in the first band a difference of 21cm^{-1} between both bands can be seen. This difference seems to be enough to discriminate between both compounds, but in the analyzed spectrum (Figure 5, spectrum a) the band appears at 705cm^{-1}, thus we cannot perform the differentiation of these carbonates with these two bands that can be seen in the region of 700-900cm^{-1} and we should focus on the region of 1600-4000cm^{-1}.

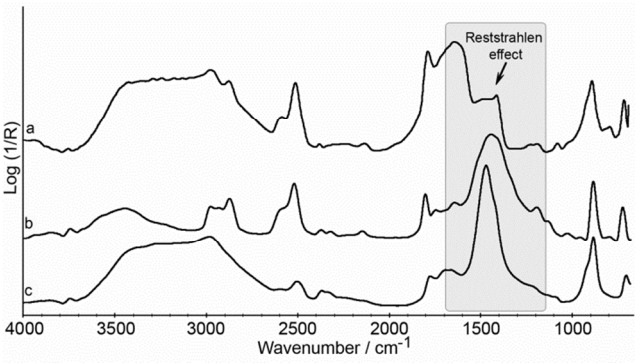

Fig. 5 a) Spectrum obtained with the handheld device in the region 4000-700cm^{-1} on calcium carbonate and sodium carbonate sample, b) DR spectrum obtained in the region 4000-700cm^{-1} on calcium carbonate sample and c) DR spectrum obtained in the region 4000-700cm^{-1} on potassium sulphate sample.

If we look at the bands that can be seen at 1784 and 2506 cm^{-1} in the analyzed spectrum (a), we can observe that it is difficult again to discern between both compounds using only these bands. In the calcite standard, two bands appear at 1794 and 2514 cm^{-1} and in the sodium carbonate standard, at 1770 and 2495 cm^{-1}, therefore, these two bands cannot be used to perform the resolution of the spectrum.

To continue, in the analyzed spectrum a shoulder at 2593 and a band at 2873cm^{-1} can be seen. This shoulder could be very important to discern between both carbonates. In the calcium carbonate standard, this shoulder is at the same wavenumber and in the standard spectrum of sodium carbonate (Figure 5, spectrum c) there is no band in that area. The same fact happens with the band at 2873 cm^{-1}, which can be seen at 2873cm^{-1} in the sodium carbonate standard, in contrast, there is no band in that area in the calcium carbonate standard. Finally, if we analyze the very broad band that can be seen around 2900-3600cm^{-1} and we compare it with the sodium carbonate standard spectrum, we could say that sodium carbonate is present in the mixed spectrum.

Finally, we could say that it is possible to discern between calcium carbonate and sodium carbonate using the FTIR handheld device when they are mixed in the same sample. We have to take into account that the resolution of this spectrum has been performed using the standards in DR mode, where the combination and overtone bands have increased their intensity. If the assignation of the spectrum of the handheld device had been performed using standards in transmittance or ATR mode the task would have been almost impossible, since the key to discern between them would be the bands at 2593, 2873 and the broad band 2900-3600cm^{-1}.

The third mixed spectrum analyzed was obtained with the handheld device on a sodium nitrate and sodium sulphate sample. In Figure 6, the obtained spectrum (a) shows the following IR bands: 727, 837, 1787, 2100, 2240, 2294, 2436, 2503, 2756 and 2844 cm^{-1} outside the region distorted by the Reststrahlen effect.

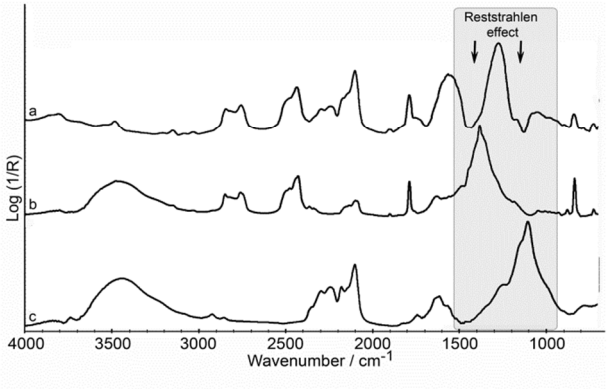

Fig. 6 a) Spectrum obtained with the handheld device in the region 4000-700cm^{-1} on sodium nitrate and sodium sulphate sample, b) DR spectrum obtained in the region 4000-700cm^{-1} on sodium nitrate sample and c) DR spectrum obtained in the region 4000-700cm^{-1} on sodium sulphate sample.

The inverted bands created by the Reststrahlen effect around 1400 cm^{-1} and 1100 cm^{-1} suggest the presence of a nitrate and sulphate compounds and the use of the overtones and combination bands will be completely necessary to perform the correct assignation. As has happened in the previous cases, the spectrum obtained with the handheld device is distorted and the region around 950-1600 cm^{-1} is not useful to perform the resolution of the spectrum. The bands that can be seen at 727, 837, 1787, 2100, 2436, 2503, 2756 and 2844 cm^{-1} belongs to the sodium nitrate and the bands at 2240 and 2294 cm^{-1} to the sodium sulphate. As it has been mentioned in the first example, it is very likely to have some areas where the bands of the two compounds overlap and at 2100 cm^{-1} this overlapping can be seen. In this example, the band at 1600 cm^{-1} could be used to resolve the spectrum, but, in our opinion, it is too close to the Reststrahlen effect and could let us to make an incorrect assignation when unknown samples are analyzed.

Finally, in the middle of the Reststrahlen area around 1300cm^{-1} we can see a band that could generate confusions. We could think that it is a typical IR spectrum and the analyzed compound has the main band at 1300 cm^{-1}, but as we have seen in the 3.2 section, these bands are usually related to weak bands that can be seen near the main bands of the analyzed compound, which have suffered an inversion in the spectra obtained with the handheld device. In this case, the band at 1300 cm^{-1} is related with the shoulder that can be seen at the same wavenumber in the sodium sulphate standard spectrum. Therefore, we have to be very careful when we analyze the region between 900-1500 cm^{-1}.

The last mixed spectrum analyzed was obtained with the handheld device on a calcium carbonate and sodium nitrate sample. In Figure 7, the obtained spectrum (a) shows the following IR bands: 716, 842, 872, 1791, 2096, 2139, 2437, 2510, 2757, 2855 and 2976 cm^{-1} outside the region distorted by the Reststrahlen effect

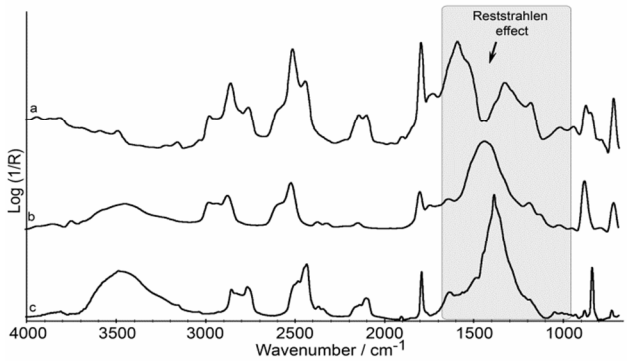

Fig. 7 a) Spectrum obtained with the handheld device in the region 4000-700cm^{-1} on calcium carbonate and sodium nitrate sample, b) DR spectrum obtained in the region 4000-700cm^{-1} on calcium carbonate sample and c) DR spectrum obtained in the region 4000-700cm^{-1} on sodium nitrate sample.

In this case again, apart from the distortions presented in the spectrum, we can see some areas where the bands of the two compounds are overlapped, which make more difficult the resolution of the spectrum. The band that can be seen at 716 cm^{-1} is the combination of the bands present at 711 cm^{-1} in the calcium carbonate standard and at 725 cm^{-1}in the sodium nitrate standard. The same happens with the bands at 842, 872, 1791 and 2855 cm^{-1}, as these four bands are the combination of both compounds and they are not useful to discern between both compounds. In contrast, the bands at 2437 and 2757 cm^{-1} belong to the sodium nitrate and the bands at 2510 and 2976 cm^{-1} to the calcium carbonate.

In conclusion, we have to be very careful when we analyze samples that can show inverted bands (nitrates, sulphates and carbonates) and to resolve the spectra obtained with the handheld device, we should initially focus on areas between 700-900 cm^{-1} and 1500-4000 cm^{-1}.

4. Database in action

The table 1 presents a database of a wide selection of compounds that have been determined in previous works by our research group using the Raman spectroscopy and XRF [25-27]. The selected standard have been characterized by diffuse reflectance in order to get a complete database of materials, which are most commonly found in affected Cultural Heritage materials.

In order to check the applicability of the presented database, we decided to perform a few preliminary analyses in the Fishermen's association building (San Sebastian, Basque Country, North of Spain).

Fishermen's association building (San Sebastian, Basque Country, North of Spain)

The building was constructed in 1929 and its ground floor is built with sandstone and cement over a limestone base and the façades of the upper floors are mainly constructed with bricks.

Table 1 Compounds characterized by diffuse reflectance spectroscopy.

Compound	Formula	Bands (wavenumber/cm^{-1})
Nonahydrated aluminum nitrate	$Al(NO_3)_3 .9 H_2O$	598 (w), 1383 (s), 1630 (s) and 3412 (vs)
Aluminum sulphate	$Al_2(SO_4)_3$	437 (w), 603 (s), 923 (w), 1103 (vs), 1633 (s), 2475 (w), 2996 (s) and 3364 (s)
Ammonium sulphate	$(NH_4)_2(SO_4)$	615 (vs), 1116 (vs), 1402 (vs), 1633 (w) and 3143 (vs)
Lead (II) sulphate	$PbSO_4$	419 (w), 601 (s), 630 (s), 967 (w), 1083 (vs), 1176 (vs), 1417 (w), 1555 (w) and 3465 (w)
Lead (II) nitrate	$Pb(NO_3)_2$	430 (vw), 580 (vw), 723 (s), 806 (w), 1016 (vw), 1075 (vw), 1127 (vw), 1376 (vs), 1631 (w), 1769 (w), 2397 (w) and 3456 (s)
Iron (II) sulphate	$FeSO_4$	615 (vs), 1096 (vs), 1624 (vs), 2330 (s) and 3321 (vs)
Nonahydrated Iron (II) nitrate	$Fe(NO_3)_2.9H_2O$	471 (vw), 826 (w), 1382 (vs), 1618 (s), 1761 (w), 2398 (w), 3352 (vs) and 3756 (vw)
Calcium carbonate	$CaCO_3$	588 (w), 711 (s), 873 (s), 1015 (vw), 1183 (w), 1434 (vs), 1635 (vw), 1794 (s), 2140 (vw), 2314 (vw), 2365 (vw), 2514 (s), 2868 (s), 2972 (s), 3443 (s) and 3741 (w)
Tetrahydrated calcium nitrate	$Ca(NO_3)_2.4H_2O$	568 (s), 827 (w), 1046 (w), 1357 (vs), 1418 (s), 1637 (s), 2135 (w), 2385 (w) and 3422 (s)
Dihydrated calcium sulphate	$CaSO_4 .2H_2O$	440 (w), 601 (s), 669 (s), 1142 (vs), 1620 (s), 1683 (s), 2131 (w), 2231 (w), 3401 (s) and 3548 (s)
Hexahydrated magnesium nitrate	$Mg(NO_3)_2 .6H_2O$	640 (s), 1383 (s), 1641 (s), 2393 (w) and 3393 (vs)
Magnesium sulphate	$MgSO_4$	425 (s), 503 (w), 615 (vs), 695 (vw), 1099 (vs), 1178 (w), 1237 (w), 1542 (w), 1650 (s), 2360 (s), 3383 (vs) and 3738 (w)
Potassium nitrate	KNO_3	824 (vs), 985 (w), 1116 (w), 1364 (vs), 1490 (s), 1760 (s), 1881 (w), 2066 (s), 2145 (w), 2396 (s), 2477 (w), 2736 (s), 2776 (s), 3101 (w), 3426 (w) and 3742 (w)
Potassium sulphate	K_2SO_4	451 (w), 616 (vs), 730 (w), 987 (w), 1117 (vs), 1227 (w), 1555 (w), 1605 (w), 2083 (s), 2138 (w), 2210 (w), 2266 (w) and 3434 (w)
Sodium carbonate	Na_2CO_3	556 (w), 623 (w), 690 (vw), 870 (s), 1458 (vs), 1652 (w), 1765 (w), 2361 (w), 2495 (w), 3975 (s) and 3741 (w)
Sodium nitrate	$NaNO_3$	725 (w), 835 (s), 876(w), 1382 (vs), 1787 (s), 2098 (w), 2429 (s), 2761 (w), 2849 (w) and 3480 (s)
Sodium sulphate (thenardite)	Na_2SO_4	414 (s), 617 (vs), 1104 (vs), 1614 (s), 1740 (w), 210 (s), 2179 (w), 2243 (w), 2296 (w), 2858 (vw), 2925 (vw), 3449 (s) and 3740 (w)
Silicium oxide (quartz)	SiO_2	466 (vs), 518 (w), 791(vs), 1055 (s), 1105 (vs), 1520 (w), 1606 (w), 1684 (w), 1793(w), 1874(s) and 1990 (w)
Titanium oxide (rutile)	TiO_2	428 (s), 674 (vs), 1073 (s), 1232 (s), 1633 (w) and 3335 (s)
Calcium oxalate monohydrate (whewelite)	$CaC_2O_4 . H_2O$	421 (w), 517 (s), 669 (s), 784 (vs), 884 (w), 949 (w), 1321 (vs), 1386 (w), 1460 (w), 1488 (w), 1627 (vs), 1906 (w), 2303 (w), 3061 (w), 3256 (w), 3336 (w), 3429 (w) and 3487 (w)

The building is located in front of an industrial harbour and the back side is adjacent to a hill, which has produced many structural problems. Moreover, when the rains are abundant, the infiltration water gets through the wall causing a high degradation in the constituent materials of the wall, since the water probably contains significant concentrations of soluble salts coming from soil leaching[28].

Nowadays, this building is classified as to be protected due to its emblematic value. Therefore, during the process of rehabilitation the façades and balcony must be restored and protected.

The visual study allowed the identification of different pathologies as efflorescence, flaking, disgregations and alveolizations. The most affected areas were the central façade and the adjacent hill wall of the ground floor. Hence, in order to test the effectiveness of the presented database to perform the identification of the spectra obtained with the handheld device, some analyses were performed on these areas.

The first series of measurements were made on decayed sandstone and the appearance of the surface of the sample suggested that the spectra obtained would be distorted due to the presence of specular and diffuse components. These analysis suggested the presence of carbonate and sulphate compounds since two inverted bands, created by the Restshtralen effect, can be seen in the range of 1000-1500cm^{-1} in Figure 8 spectrum a.

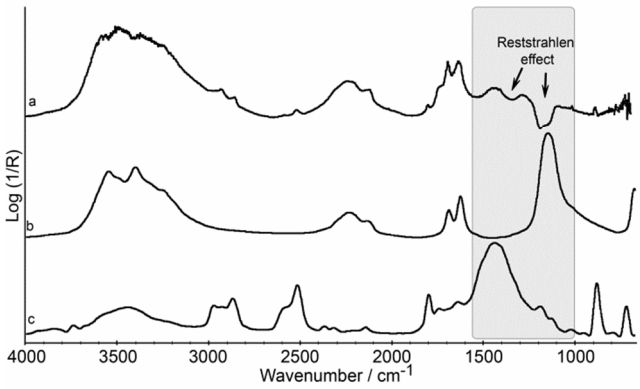

Fig. 8 a) Spectrum obtained with the handheld device in the region 4000-700cm^{-1} taken with the portable device on a white efflorescence of the Fishermen's Association building in San Sebastian, b) DR spectrum obtained in the region 4000-700cm^{-1} on calcium sulphate dehydrated sample and c) DR spectrum obtained in the region 4000-700cm^{-1} on calcium carbonate sample.

Owing to the distortions observed in the spectrum, the assignment of calcite, by the main absorption band, was impossible. As was mentioned in the previous section, the elucidation of the spectrum obtained with the handheld device was performed using standards, in DR mode. The assignment of the calcium carbonate was performed with the bands observed at 873, 1794, 2514, 2868 and 2972 cm^{-1}. Apart from that, the second compound detected was calcium sulphate dehydrated, which was assigned by the bands presented at 1620, 1683, 2122 and 2231cm^{-1}.

Some analyzed areas gave more complex spectra than that shown in Figure 8. An example is the spectrum of Figure 9, obtained from a decayed sandstone material. In this case, the Reststrahlen effect appeared in two different ranges at 1000-1100 cm^{-1} and at 1400-1500 cm^{-1}.

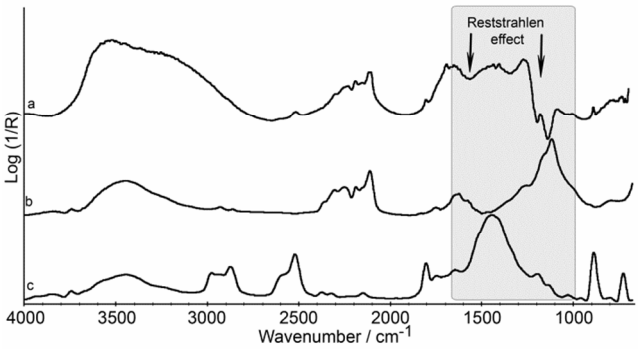

Fig. 9 a) Spectrum obtained with the handheld device in the region 4000-700cm^{-1} taken with the portable device on a white efflorescence of the Fishermen's Association building in San Sebastian, b) DR spectrum obtained in the region 4000-700cm^{-1} on potasium sulphate sample and c) DR spectrum obtained in the region 4000-700cm^{-1} on calcium carbonate sample.

These two inverted bands at those wavenumbers suggested that sulphates and carbonates could be present due to their main stretching vibrations are observed at those spectral regions. However, it was impossible to perform a clear assignment based on such bands due to the distortion of the spectrum. Thus, the identification of these compounds required once more the use of the secondary bands (combination and/or overtones). In this way, the assignment of the calcium carbonate was performed by the bands at 873, 1794 and 2514 cm^{-1}. In this sample, the signal of the calcium carbonate was much lower than the signals that we have obtained in the laboratory examples. The second compound characterized was the sodium sulphate and the identification was carried out by the bands observed at 2101, 2179 and 2243 cm^{-1}.

Finally, in a white efflorescence found in the adjacent wall of the hill, some analyses were performed obtaining the response that can be seen in Figure 10, spectrum a. The comparison with the DR spectra of pure standards lead to the identification of two compounds: (I) potassium nitrate due to the match of eight bands at 842, 1761, 2394, 2735, 2779, 3103, 3426 and 3745cm^{-1} (see Figure 10, spectrum b) and (II) calcium sulphate (as gypsum form, $CaSO_4.2H_2O$) using the bands at 1620, 1683 and 2231cm^{-1} (see Figure 10, spectrum c).

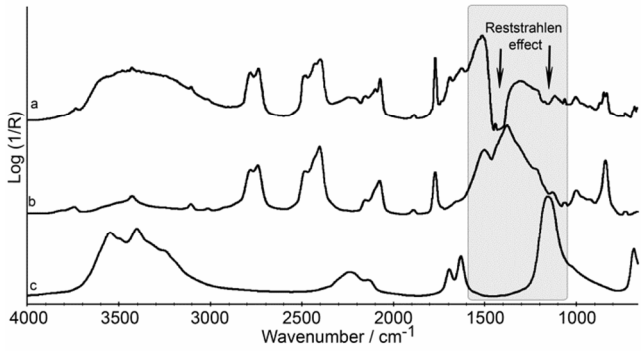

Fig. 10 a) Spectrum obtained with the handheld device in the region 4000-700cm^{-1} taken with the portable device on a white efflorescence of the Fishermen's Association building in San Sebastian, b) DR spectrum obtained in the region 4000-700cm^{-1} on potassium nitrate sample and c) DR spectrum obtained in the region 4000-700cm^{-1} on calcium sulphate dehydrated sample.

Analyzing the results from the conservation state point of view, it is obvious that the Fishermen's association building ground floor is clearly impacted by soluble salts. The crystallization of soluble salts into the building materials is considered one of the most destructive processes of deterioration as they can cause different pathologies when they crystallize/dissolve within the pores and capillaries networks[29-31]. For this reasons, the characterization of salts found in the materials is crucial to diagnose the chemical process of the deterioration. Currently, this type of study is increasingly required prior to any conservation interventions.

Therefore, this work shows a useful applicability that this technique could have in the diagnosis of pathologies that the Built Heritage can suffer. Thus, the main aim of the work is achieved, i.e. to show the application of the presented database in DR mode and to demonstrate that with the standards in DR mode the spectra obtained with the handheld device on Building materials could be resolved in a straightforward manner.

5. Conclusions

In-situ analyses are conditioned by external factors that are difficult to control and very often the spectra obtained are of poorer quality, which makes their resolution more difficult. To the problems that could be found in the measurement process, we have to add the distortions present in the spectra when samples, which contain oxyanions, such as, nitrates, carbonates and sulphates are analyzed. These distortions make even more difficult the resolution of the in-situ spectra obtained, but if we analyze the literature, we can find several work that use this handheld device to analyze Cultural Heritage materials with successful results. This portable handheld spectrometer has been used to characterize and diagnose the conservation state of the building materials of the Guevara Palace (15th century, Segura, Basque Country, Spain) and different 19th century wallpapers manufactured by the Santa Isabel factory (Vitoria-Gasteiz, Basque Country, Spain) and by the Dufour and Leroy manufacturers (Paris, France)[13]. It also has been used to study the dissolution process of weathering steel in urban areas and to analyze two wall paintings located in Saint Andrew Church (Biañez, Biscay) and Saint John the Baptist Church (Axpe, Biscay) [14,16]. Therefore, this handheld device could be very useful to analyze any material related with the Cultural Heritage despite the limitations that we have analyzed in the presented work.

Finally, in our opinion, the preliminary DR database presented in this work is the best tool to perform the resolution of the spectra obtained with the handheld device on building materials, showing the powerful usefulness that this technique can bring to the field of the study of pathologies suffered by Cultural Heritage.

Acknowledgments

This work has been performed under projects DEMBUMIES (ref. BIA2011-28148) funded by the Spanish Ministry of Economy and Competitiveness (MINECO) and UFI Global Change and Heritage (ref UFI11-26) funded by the UPV/EHU. Iker Arrizabalaga, Olivia Gómez-Laserna and Azibar Rodriguez acknowledge their predoctoral grants from the UPV/EHU.

Notes and references

Department of Analytical Chemistry, University of the Basque Country UPV/EHU, P.O. Box 644, E-48080 Bilbao, Basque Country, Spain
Tel.:+34 94 601 82 94; fax:+34 94 601 35 00
E-mail: iker.arrizabalaga@ehu.es

1 K. Castro, N. Proietti, E. Princi, S. Pessanha, M.L. Carvalho, S. Vicini, D. Capitani and J.M. Madariaga, Anal Chim Acta, 2008, **623**, 187-194
2 O. Gómez-Laserna, M.A. Olazabal, H. Morillas, N. Prieto-Taboada, I. Martinez-Arkarazo, G. Arana and J.M. Madariaga J. Raman Spectrosc, 2013, **44**, 1277–1284
3 L. Appolonia, D. Vaudan, V. Chatel, M. Aceto and P. Mirti, Anal Bioanal Chem, 2009, **395**, 2005–2013
4 E. Cheilakou, M. Troullinos and Maria Koui, J Archaeol Sci, 2014, **41**, 541-555
5 A. Pallipurath, J. Skelton, P. Ricciardi, S. Bucklow and S. Elliotta, J. Raman Spectrosc, 2013, **44**, 866–874
6 T. Poli, O. Chiantore, M. Nervo and A. Piccirillo, Anal Bioanal Chem, 2011, **400**, 1161–1171
7 T. Poli, A. Elia and O. Chiantore, e-Preservation Science, 2009, **6**, 174-179
8 T. Armaroli, T. Bécue, T. Gautier, Oil & Gas Sci Technol 2004, **59**, 215-237
9 C.Ricci, C. Miliani and B.G. Brunetti, A. Sgamellotti, Talanta, 2006, **69**, 1221–1226
10 D. Buti, F. Rosi, B. G. Brunettiand C. Miliani, Anal Bioanal Chem, 2013, **405**, 2699–2711

11 L. Monico, F. Rosi, C. Miliani, A. Daveri and B.G. Brunetti, Spectrochim Acta Part A, 2013, **116**, 270-280

12 C. Miliani, F. Rosi, F. Daveri and B.G. Brunetti, Appl Phys A, 2012, **106**, 295-307

13 I. Arrizabalaga, O. Gomez-Laserna, J. Aramendia, G. Arana and J.M. Madariaga Spectrochim Acta Part A, 2014, **129**, 259–267

14 M. Irazola, M. Olivares, K. Castro, M. Maguregui, I. Martínez-Arkarazo, J. M. Madariaga, J. Raman Spectrosc. 2012, **43**, 1676–1684

15 J.M. Colwell, J.H. Khan, A. Harman, A. Trueman, G. McAdam, G.A. George, G. Will, International Corrosion Congress, 18th, Perth, Australia, 2011, **2**, 1070-1081.

16 J. Aramendia, L. Gomez-Nubla, I. Arrizabalaga, N. Prieto-Taboada, K. Castro, J.M. Madariaga, Corros Sci, 2013, **76**, 154–162

17 I. Arrizabalaga, O. Gomez-Laserna, J. Aramendia, G. Arana and J.M. Madariaga Spectrochim Acta Part A, 2014, 124, 308–314

18 C.E. Silva, L.P. Silva, H.G.M. Edwards and L.F. De Oliveira, Anal Bioanal Chem, 2006, **386**, 2183–2191

19 K. Qiu, X. Song, Y. Lai, L. Wu, G. Tang and S. Min, Anal. Methods, 2013, **5**, 4790–4797

20 N.J. Harrick and F.K. du Prè, Applied Optics, 1966, **11**, 1739-1743.

21 L.A. Averett, P.R. Griffiths and K. Nishikida, J Anal Chem, 2008, **80**, 3045–3049.

22 E.L. Kendix, S. Prati, E. Joseph, G. Sciutto and R. Mazzeo, Anal Bioanal Chem, 2009, **394**, 1023–1032

23 E. Ruiz-Agudo, B. Lubelli, A. Sawdy, R. Van Hees, C. Price and C. Rodriguez-Navarro, Environ Earth Sci, 2011, **63**, 1475-1486

24 C. Milliani, F. Rosi, B.G. Brunetti and A. Sgamelloti, Accounts Chem Res, 2010, 43, 728-738

25 H. Morillas, M. Maguregui, O. Gómez-Laserna, J. Trebolazabala and J.M. Madariaga, J. Raman Spectrosc (2013), **44**, 1700–1710

26 O. Gómez-Laserna, M. Olazabal, H. Morillas, N. Prieto-Taboada, I. Martinez-Arkarazo, G. Arana and J.M. Madariaga, J. Raman Spectrosc, (2013), **44**, 1277–1284

27 M. Irazola, M. Olivares, K. Castro, M. Maguregui, I. Martinez-Arkarazo and J.M. Madariaga, J. Raman Spectrosc, 2012, **43**, 1676–1684

28 V. Matović, S. Erić, A. Kremenović, P. Colomban, D. Serćković-Batoćanin and N. Matović, J. Cult. Herit, 2012, **13**, 175-186

29 L. Dei, M. Mauro and G. Bitossi, Thermochim Acta, 1998, **317**, 133-140

30 N. Thaulow and S. Sahu, Mater Charact, 2004, **53**, 123-127

31 R.M. Espinosa-Marzal and G.W. Scherer, Accounts Chem Res, 2009, **43**, 897-905